Quality Assurance and Safety of Crops & Foods, 2017; 9 (4): 463-478

Wageningen Academic Publishers

Modelling some engineering properties of walnut kernel undergoing different drying methods with microwave pre-treatment

M. Jafarifar, R.A. Chayjan*, N. Dibagar and B. Alaei

Department of Biosystems Engineering, Faculty of Agriculture, Bu-Ali Sina University, 6517833131, Hamedan, Iran; amirireza@basu.ac.ir

Received: 2 January 2017 / Accepted: 1 June 2017

RESEARCH ARTICLE

Abstract

This work aimed in modelling some physical and thermal properties of walnut kernel undergoing various drying techniques include microwave semi-industrial continuous drying (M-CD), microwave infrared-vacuum drying (M-IVD), and microwave infrared-fluidised bed drying methods. By using the verifications of experimental parameters, ten drying models for describing combined effects of independent variables were derived and the parameters of these models were determined by multiple regression analysis. In the case of the model, comprised of collective effects of drying independents, the Midilli model gave the best result in describing drying behaviour of walnut kernel in all experimental domains. Minimum values of shrinkage (6.53%) and colour change (5.54%) were obtained in the M-CD with the microwave power of 270 W, air temperature of 45 °C, and belt linear speed of 10.5 mm/s, however maximum shrinkage (14.65%) and colour change (18.28%) were related to the M-IVD with microwave power of 630 W, drying temperature of 75 °C, and absolute pressure of 60 kPa. The lowest and highest values of effective moisture diffusivity (1.04×10^{-8} and 9.74×10^{-8} m^2/s, respectively) belonged to the M-CD. Based on the quality indices including shrinkage and total colour difference M-CD was found an adequate arrangement among applied techniques in walnut kernel drying, hence it produced the most similar dried samples to fresh ones.

Keywords: walnut kernel, drying modelling, shrinkage, total colour difference, diffusivity

1. Introduction

Persian walnut (*Juglansregia* L.) as a horticultural crop is one of the most important members of the nuts family cultivated in the temperate regions and northern hemisphere (Khadivi-Khub *et al.,* 2015). Walnut is native to the mountain ranges of Central Asia from Xinjiang province of western China to eastern Turkey and this extending includes countries like Uzbekistan, India, Pakistan, and Iran (Pollegioni *et al.,* 2014). The walnut fruit has a high nutritional value and it is rich in oil composed of unsaturated fatty acids (60-75%) including other compounds such as high biological-value proteins (up to 15% of the kernel mass), carbohydrates (12-16%), fibre (up to 2.1%), followed by vitamins (A, B, C, D) and trace minerals (calcium, iron, etc.) (USDA, 2015). Based on statistics, Iran with producing 450,000 tons of walnut per year after the mainland of China has the most production in the world (FAO, 2012).

Initial moisture content of fresh walnut kernel is about 35-40% (dry basis). To maintain the oil content and prevent corruption, the final moisture content should attain to about 4-8% (dry basis) after harvesting (Ghatrehsamani and Zomorodian, 2012). Thus, developing an appropriate harvesting and post-harvest handling method is a major concern in the nut industry (Kouchakzadeh, 2013). Similar to other nuts and beans, drying or dehydration is one of the common methods of walnut processing. Drying stabilises the product mass, prevents kernel quality loss by diminishing the moisture content and water activity of biological material, improves bleaching efficiency and prolongs storage life (Monteiro *et al.,* 2015).

New tendencies in the development and progression of processes and products dehydration eventuate to the arrangement of different conventional and non-conventional drying technologies. To defeat the restrictions of slow drying

processes, microwave (MW) drying can significantly shorten the drying process by the goodness of individual profits. The unique heating mechanism of MW, which involves heating a food material inside out based on its dielectric properties, makes it applicable in drying operation. The application could be at various drying stages such as pre, post, and during drying. To save energy and avoid risk of overheating, it is possible to apply MW field intermittently and such a scheme can be carried out with airflow or under vacuum conditions. Exposing a moist material to the MW energy before main drying course causes the inner moisture to get heated up and migrate to the surface due to the pressure differential for subsequent drying by other methods such as vacuum or hot air drying (Zhang *et al.*, 2006). Structural modification has also been reported in MW heating as pre-treatment for drying (Rodríguez and Lombranna, 2007). The added advantage of this is quick drying as well as reduction in shrinkage, loss of water-soluble components, and energy savings. Many researchers have successfully dried vegetables and fruits with employing MW in conjunction with other drying methods, such as in combination with continuous dryer for apple (Ahrne *et al.*, 2003), potato (Ahrne *et al.*, 2003), kiwifruit (Maskan, 2001), olive (Gogus and Maskan, 2001). This combination mainly caused rapid reduction of surface moisture and consequent shrinkage, which often results in reduced moisture transfer and, sometimes, reduced heat transfer (Monteiro *et al.*, 2015). To provide thermal energy needed for water evaporation, MW-assisted combination drying with vacuum has been investigated to speed up the process (Gonçalves *et al.*, 2016). In particular, MW-assisted vacuum drying techniques are reported to be used successfully for the dehydration of grapes (Clary *et al.*, 2005), tomatoes and bananas (Durance and Wang, 2002), carrots (Cui *et al.*, 2005). In addition, an accelerating dehydration rate period existed in the initial period during combine far-infrared microwave drying of peach (Wang, and Sheng, 2006).

Mathematical modelling of drying kinetics of food products allows describing the drying behaviour and quality characteristics of product in a thin layer dryer. Analysis of drying curves provides better understanding of drying process to choose the best drying condition (Aregbesola *et al.*, 2015). Exponential models are usually used to determine thin layer drying characteristics of agricultural products (Koukouch *et al.*, 2015; Rodriguez *et al.*, 2005). In recent years, some studies about mathematical modelling of combined drying processes were published (Aidani *et al.*, 2016; Faal *et al.,* 2015). The objectives of this work were to study and modelling some physical and thermal properties of walnut kernel dehydration in convective, infrared-vacuum and infrared-fluidised bed dryers, all with microwave pre-treatment. The predictive models can be applied as a tool for determination of process time, process control or evaluation of the effect of modifications in the process variables.

2. Materials and methods

Sample preparation

Fresh walnut (*Juglans* species, Toyserkani cultivar) was used as raw material in this study. In mid-September immediately after walnut plucking, those with a green husk were packed in the vacuum bags and stored in a refrigerator at 4 °C to prevent moisture loss and reduce spoilage until later use. Before drying process, samples were taken out of the refrigerator and after removing unripe and damaged kernels, walnuts of uniform size were selected. After peeling the green husk, to eject the spherical kernel from the shell without physical damages, the wooden shell was broken with great precision. The weight of each experimental unit was about 100 gr. The geometric mean diameter of the kernels was 33.02±8 mm. The walnut moisture content was determined by the gravimetric method utilising an oven at 105±1 °C and an analytical electrical balance (AND GF 6000, , A&D Company Limited, Tokyo, Japan) with an accuracy of 0.001 g (Togrul *et al.*, 2007). Initial moisture content of walnut kernel was obtained 0.48 (dry basis). Walnut samples were dried to a mean final moisture content of 0.05 (dry basis). These samples were cooled to the ambient temperature, then packed in polyethylene bags and stored at 4 °C for evaluation of drying specifications. In all experiments, ambient air temperature, and air relative humidity were measured and recorded 25 to 31 °C and 22 to 27%, respectively. Each experiment was performed in triplicate.

Experimental setup

For this research, three different drying technologies were investigated. Microwave oven, semi-industrial continuous, infrared-vacuum, and infrared-fluidised bed dryers were the common experimental setups, which were developed to perform the drying process in the Biosystems Engineering Department of Bu-Ali Sina University, Hamedan, Iran. A programmable household microwave oven (Sharp, R-I96T, Sharp Co. Ltd., Bangkok, Thailand) with a maximum output of 900 W was employed as pre-treatment setup for drying experiments.

The main parts of CD include metal walls with Polyurethane thermal insulation and thickness of 5 cm. Entrance and exit doors were covered by double glass insulation. Wide Polyvinyl chloride conveyor was considered for sample transfer and belt shaft followed by an electrical heater (16×300 W heating elements), air blower with an electrical motor of 1 hp, a power transmission system for conveyor belt with the ratio of 1:100 and electrical motor of 0.75 kW are contained in the continuous dryer. Electrical control panel board includes all keys of different parts, air velocity inverter (Delta S1, Delta Electronics, Beijing, China), belt speed inverter (Delta VFD-B, Delta Electronics, Beijing,

China), voltage display and thermostat (Atbin 400k, Atbin Co., Tehran, Iran) (Figure 1).

Schematic view of a lab-scale IVD is shown in Figure 2. The set of connections was fabricated from a hollow cylinder made of Teflon as drying chamber. To provide the necessary heat and infrared power for drying, the top of the chamber was equipped with an infrared lamp (100 W). The air temperature near the sample tray in the dryer was recorded using a thermometer with type k sensor with an accuracy of 0.1 °C (Lutron TM-903, Lutron Electronic Enterprise Co. Ltd., Taiwan). To create vacuum condition in drying chamber, a vacuum pump (DV-285N-250-Platinum, JB Industries, Aurora, IL, USA) connected to the chamber through high-pressure pipes. Electrical control system consists of a thermostat (Atbin 400k) to control the temperature inside the chamber and pressure controller (Sensys PSCH0001 BCIJ, Sensor System Technology Co. Ltd., Geyonggi-Do, Korea) to control absolute pressure during each experiment with accuracy of ±0.001 bar.

Figure 3 demonstrates a schematic view of IFD. This set up also consisted of a metal chamber with glass wool insulation, 4×500 W infrared lamps (Philips 500 W, Philips Company, Wommelgem, Belgium) installed inside the drying chamber, electrical heaters (8×300 W heating elements), air manufacturing system (centrifugal blower with 1.5 hp electrical motor), electrical control panel board including all control keys of infrared lamps and different parts of dryer, inverter (VFD-M, Delta Electronics Inc., Taiwan) of blower and thermostat (Atbin 400k) to control the input air temperature. A hygrometer (with accuracy of 3% RH) was employed to measure the air relative humidity. Furthermore, to measure the sample dimensions, a digital caliper (General Ultratech EDF-6, General Tools & Instruments LLC., Secaucus, NY, USA) with accuracy of 0.01 mm was used. Walnut kernels were weighed once all three minutes using a weighting system contained an electronic balance.

Experimental procedure

The walnut samples were initially subjected to the MW radiation as a pre-treatment (for 20 seconds) in power levels of 270, 450 and 630 W then exposed to the different drying setups to reach the final moisture content of 5% (dry basis). The pre-treatment by MW radiation was carried out before each run in three main drying domains up to the end of the experiments. Trails in semi industrial continuous domain were conducted in the air temperatures of 45, 60 and 75 °C, and belt linear speeds of 2.5, 6.5 and 10.5 mm/s. Air velocity was considered about 1.5 m/s in all experiments. Infrared-vacuum condition subjected to the sample in the air temperatures of 45, 60 and 75 °C, and vacuum pressures of 20, 40 and 60 kPa. Infrared-fluidised bed drying was conducted in the air temperatures of 45, 60 and 75 °C, and radiant powers of 500, 1000 and 1,500 W. In all experiments, air velocity was considered about 1 m/s. Differences between means of data were statically analysed by least significant difference and Duncan tests using the SPSS version 20 (IBM Corporation, Armonk, NY, USA).

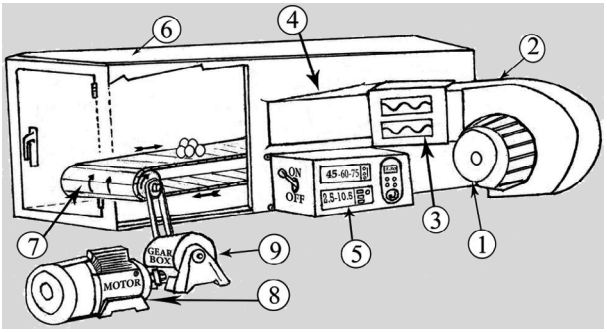

Figure 1. Schematic view of a lab scale continuous drying. 1 = blower and electrical motor; 2 = air channel; 3 = electrical heater; 4 = hot air inlet gate; 5 = air velocity and belt speed inverters and thermostat; 6 = drying chamber; 7 = conveyor belt; 8 = belt electrical motor; 9 = belt gear box.

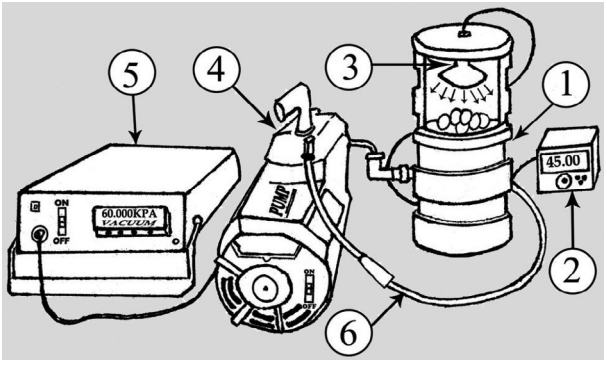

Figure 2. Schematic view of lab scale infrared-vacuum drying. 1 = drying chamber; 2 = thermostat; 3 = infrared lamp; 4 = vacuum pump; 5 = pressure controller; 6 = suction pipe.

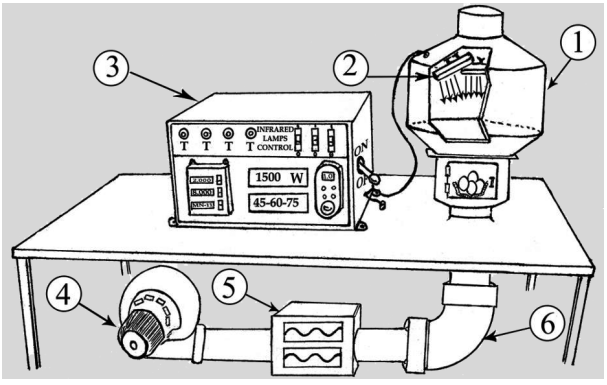

Figure 3. Schematic view of lab scale infrared-fluidised bed drying. 1 = drying chamber; 2 = infrared lamp; 3 = control unit (lamps switches, inverter and thermostat); 4 = blower and electrical motor; 5 = electrical heater; 6 = hot-air transfer pipe.

Mathematical modelling of drying kinetics

To investigate the thin layer drying characteristics of the walnut kernel, the experimental data obtained under different drying conditions were fitted with 10 assorted moisture ratios of thin-layer drying models. The moisture ratio (MR) of the walnut kernel during thin layer drying was calculated by the following Equation (Siqueira *et al.*, 2012):

$$MR = \frac{M - M_e}{M_0 - M_e} \quad (1)$$

Where MR is the moisture ratio (dimensionless), M is the moisture content of the walnut kernel ($kg_{water}/kg_{dry\ solid}$), M_0 is the initial moisture content ($kg_{water}/kg_{dry\ solid}$) and M_e is the equilibrium moisture content ($kg_{water}/kg_{dry\ solid}$). To select the best model, three criteria were determined to describe drying kinetics of walnut kernel in all experimental domains: correlation coefficient (R^2), reduced chi-square (χ^2) and root mean square error (RMSE) (Aghbashlo *et al.*, 2011).

$$R^2 = 1 - \left[\frac{\sum_{i=1}^{N} \left(MR_{pre,i} - MR_{\exp,i} \right)^2}{\sum_{i=1}^{N} \left(\overline{MR}_{pre} - MR_{\exp,i} \right)^2} \right] \quad (2)$$

$$\chi^2 = \frac{\sum_{i=1}^{N} \left(MR_{\exp,i} - MR_{pre,i} \right)^2}{N - n} \quad (3)$$

$$RMSE = \sqrt{\frac{1}{N} \sum_{i=1}^{N} (MR_{pre,i} - MR_{\exp,i})^2} \quad (4)$$

Where $MR_{exp,i}$ and $MR_{pre,i}$ are experimental and predicted moisture ratios of i^{th} data, N is the number of observations and n is the number of drying constants. $\overline{MR}_{pre}$ is the mean value of the predicted moisture ratio. Calculations of statistical parameters and all of the regression analysis were performed by MatlabV7.14.0.739 (R20129a, MathWorks, Natick, MA, USA) software.

Shrinkage

Volume changes of the biological materials during the drying process, due to water evaporation, called shrinkage (Alaei and Chayjan, 2015). Based on the measuring of primary and secondary volumes of material, shrinkage ratio (S_b) was calculated using the following formula (Janjai *et al.*, 2010).

$$S_b(\%) = \left(\frac{V_0 - V}{V_0} \right) \times 100 \quad (5)$$

Where V_0 is the initial or primary volume of the sample (m^3) and V is the secondary or final volume of the sample after drying (m^3). To calculate the primary and secondary volumes, three basic diameters (width, length, and thickness) of all walnut kernels were measured by a digital caliper with an accuracy of 0.01 mm (Nowacka *et al.*, 2012).

Colour change

In food dehydration, appearance properties such as colour are employed as indicators of food quality or visual qualitative assessment, which are very important in marketing and customer-friendly. Colour is one of the main parameters from the perspective of consumers (Lüle and Koyuncu, 2015). All of the walnut kernels were cut after drying by a sharp knife from the middle part as a perfectly smooth surface. All surfaces were scanned using a flatbed scanner (HP Scanjet G4050 Photo Scanner, HP Inc., Palo Alto, CA, USA) with resolution up to 4,800 dpi×9,600 dpi (Darrigues *et al.*, 2008).

The scanned images arrived in Adobe Photoshop CS6 software (Softonic International S.A., Barcelona, Spain) and the colour values of *L*, *a*, and *b* of all scanned images were obtained. Using the following formulas *L*, *a*, and *b* converted to L* (whiteness/darkness), a* (redness/greenness) and b* (yellowness/blueness) space (Alaei and Chayjan, 2015).

$$L^* = \frac{Lightness}{255} \times 100 \quad (6)$$

$$a^* = \frac{240\,a}{255} - 120 \quad (7)$$

$$b^* = \frac{240\,b}{255} - 120 \quad (8)$$

The total colour change (ΔE) was calculated by the following mathematical formula:

$$\Delta E = \sqrt{(L_0^* - L^*)^2 + (a_0^* - a^*)^2 + (b_0^* - b^*)^2} \quad (9)$$

Where L_0^*, a_0^* and b_0^* are the initial colour values of the samples before drying and the L^*, a^* and b^* are the final colour values of the samples after drying.

Effective moisture diffusivity and activation energy

The Fick's second law of unsteady state diffusion in spherical sample was applied to calculate the effective moisture diffusivity (Rudy *et al.*, 2015). To describe the moisture transfer during the drying process and reduce sample moisture, it was assumed that the distribution of initial moisture is constant, radial and uniform then it is calculated by the following formula (Crank, 1997).

$$MR = \frac{M_t - M_e}{M_0 - M_e} = \frac{6}{\pi^2} \sum_{n=1}^{\infty} \frac{1}{n^2} exp\left(-n^2 \pi^2 \frac{D_{eff} t}{r_0^{\,2}} \right) \quad (10)$$

Where MR is the sample moisture ratio, M_t is the moisture content at any time ($kg_{water}/kg_{dry\ solid}$), M_e is

the equilibrium moisture content (kg $_{water}$/kg $_{dry\ solid}$), M_0 is the initial moisture content (kg $_{water}$/kg $_{dry\ solid}$), $n=1,2,3,...$ ... is the number of terms taken into consideration, t is the drying time (s), D_{eff} is the effective moisture diffusivity (m^2/s) and r_0 is the radius of walnut kernel (m). Drying of walnut kernel was performed in a long time period, so Equation 10 can be simplified to first term of series only as Equation 11, without much efficacy on precision of calculations:

$$MR = \left(\frac{6}{\pi^2}\right)\exp\left(-\pi^2\frac{D_{eff}t}{r_0^{\ 2}}\right) \quad (11)$$

With simplified to a straight-line of Equation 11:

$$\ln(MR) = \ln\left(\frac{M_t - M_e}{M_0 - M_e}\right) = \ln\left(\frac{6}{\pi^2}\right) - \left(\pi^2\frac{D_{eff}t}{r_0^{\ 2}}\right) \quad (12)$$

In the microwave semi-industrial continuous drying (M-CD) domain, due to the consideration of the belt linear speed, expression of (x/u_b) can be an appropriate alternative to the drying time (t), where x is the amount of displacement of samples during drying process (m) and (u_b) is the linear speed of belt (m/s). The slope K_1 is calculated by plotting the natural logarithm of walnut kernel drying data (ln (MR)) versus drying time (t or x/u_b) depending on the dryer type) according to Equation 12. Therefore, effective moisture diffusivity can be calculated as (Crank, 1997):

$$K_1 = \frac{\pi^2 D_{eff}}{r_0^{\ 2}} \quad (13)$$

Arrhenius equation was applied to calculate the activation energy of walnut kernel drying, (Alaei and Chayjan, 2015):

$$D_{eff} = D_0\exp\left(-\frac{E_a}{RT}\right) \quad (14)$$

Where E_a is the activation energy for diffusion (kJ/mol), R is the universal gas constant (8.3143 J/mol.K), T is the absolute air temperature (K), D_0 is the pre-exponential factor of the Arrhenius equation or equivalent to the diffusivity at extremely high temperature (m^2/s). By taking natural logarithm of the Arrhenius equation, Equation 14 can be written as (Alaei and Chayjan, 2015):

$$\ln(D_{eff}) = \ln(D_0) - \left(\frac{E_a}{R}\right)\left(\frac{1}{T}\right) \quad (15)$$

A straight line by plotting ln(D_{eff}) versus 1/T with a slope of K_1 was created. K_2 can be calculated using the following equation:

$$K_2 = \frac{E_a}{R} \quad (16)$$

3. Results and discussion

Drying kinetics and mathematical modelling

Supplementary Figures S1, S2 and S3 show the typical drying curves of fresh walnut kernel at different drying conditions in M-CD, microwave infrared-vacuum drying (M-IVD) and microwave infrared-fluidised bed drying (M-IFD) domains, respectively. The general characteristic of these curves seen in figures is their resemblance as being typical drying curve. Based on figures, the moisture content decreased exponentially with drying time. Drying temperature and microwave power significantly affected the moisture change of fresh walnut kernel. In all experimental domains by increasing drying temperature and microwave power within the study range, the amount of moisture removed from the walnut kernel increased and the time required achieving final moisture content in products diminished. It can be attributed to the increasing temperature gradient between drying product and its surrounding. In addition, increased drying temperature and microwave power caused more energy transfer to the walnut kernel eventuated to the improved evaporation intensity as well as augmented moisture diffusivity. Another factor in M-CD domain contributed to the increasing drying rate was increasing the belt linear speed from 2.5 to 10.5 mm/s. In higher linear speeds, belt reaches to the end of its movement cycle sooner than lower speeds; therefore, the number of microwave treatments before each run and consequently the exposure time of samples to the microwave radiation were longer. This causes more heat generation when microwave interacts with the polar water molecules in product and a significantly high drying rate was achieved when compared with lower belt linear speeds. In M-IVD, by reducing the absolute pressure from 60 to 20 kPa, drying time decreased. This phenomenon can be attributed to the decrease in the saturation temperature and related absolute pressure of water and increased drying rate. In infrared-fluidised bed system, increasing the radiant power from 500 to 1,500 W (by increasing the number of infrared lamps) drying rate increased, as well. This was because of an augmentation in the infrared intensity led to an increase in the infrared energy absorbed by product. In general, the time required to reduce the moisture content to any given value was dependent on the drying conditions, being highest at infrared power of 300 W, air temperature of 35 °C and air velocity of 1.5 m/s and lowest at infrared power of 500 W, air temperature of 45 °C and air velocity of 1.0 m/s. Based on results, the maximum drying time (about 100 min) in M-CD of walnut kernel was obtained in the microwave power of 270 W, air temperature of 45 °C, and belt linear speed of 2.5 mm/s and minimum drying time (about 11 min) was achieved in microwave power of 630 W, air temperature of 75 °C, and belt speed of 10.5 mm/s. Maximum drying time (about 86 min) in M-IVD belonged to the 630 W, 75 °C, and 20 kPa however, minimum drying

time (about 16 min) was related to the condition of 270 W, 45 °C, and 60 kPa. Also, the microwave power of 270 W, air temperature of 45 °C, and radiant power of 500 W led to maximum drying time (about 70 min) in M-IFD, while the microwave power of 630 W, air temperature of 75 °C and radiant power of 1,500 W resulted in minimum drying time (about 22 min).

The experimental data of dimensionless moisture content from various drying experiments were converted into MR using MATLAB software and then they were fitted by means of ten different thin-layer drying models that are widely used in most foods and biological materials (Table 1). These models were appraised to find the best models for estimation of the walnut drying behaviour. Considering values of comparison indices including correlation coefficient (R^2), residual mean square error (RMSE) and chi square (χ^2), different empirical models were examined and the best model was selected based on the criteria of the maximum R^2, minimum RMSE and χ^2 in all experimental domains.

The models were fitted to the experimental data and evaluation was performed utilising the goodness of statistical results. The values of three main indicators in different drying conditions are presented in Table 2. As it can be seen, the Midilli model with R^2=0.9927, RMSE=0.0260 and χ^2=0.0100 in continuous, R^2=0.9918, RMSE=0.0305 and χ^2=0.0095 in infrared-vacuum and R^2=0.9917, RMSE=0.0293 and χ^2=0.0105 in infrared-

Table 1. Mathematical models applied to drying data.

Models name	Model equation[1]	References
Newton or Lewis	$MR=\exp(-kt)$	Kashaninejad *et al.*, 2007
Page	$MR=\exp(-kt^n)$	Crank, 1997
Wang and Singh	$MR=1+ at+bt^2$	Wang *et al.*, 2015
Henderson and Pabis	$MR=a \exp(-kt)$	Wang and Sheng, 2006
Midilli	$MR=a \exp(-kt^n)+bt$	Alaei and Chayjan, 2015
Aghbashlo	$MR=\exp(-at/(1+bt))$	Wang *et al.*, 2015
Logistic	$MR=c/(1+a \exp(kt))$	Crank, 1997
Thompson	$MR=\exp((-a-(a^2+4bt)^{0.5})/2b)$	Dash *et al.*, 2013
Diffusion approach	$MR=a \exp(-kt)+(1-a) \exp(-kbt)$	Siqueira *et al.*, 2012
Modified Henderson and Pabis	$MR=a \exp(-kt)+b \exp(-gt)+c \exp(-ht)$	Janjai *et al.*, 2010

[1] Where t is drying time; a, b, c, n are models coefficients and k, g, hare drying constants; MR = moisture ratio.

Table 2. Results of statistical analysis on ten mathematical drying models.[1]

Models name	Dryer type								
	M-CD			M-IVD			M-IFD		
	R^2	RMSE	χ^2	R^2	RMSE	χ^2	R^2	RMSE	χ^2
Newton or Lewis	0.9868	0.0319	0.0187	0.9813	0.0393	0.0221	0.9890	0.0302	0.0140
Page	0.9909	0.0270	0.0124	0.9889	0.0317	0.0131	0.9905	0.0288	0.0120
Wang and Singh	0.9888	0.0296	0.0161	0.9876	0.0335	0.0165	0.9870	0.0340	0.0174
Henderson and Pabis	0.9878	0.0315	0.0170	0.9825	0.0396	0.0201	0.9898	0.0299	0.0128
Midilli	0.9927	0.0260	0.0100	0.9918	0.0305	0.0095	0.9917	0.0293	0.0105
Aghbashlo	0.9914	0.0261	0.0117	0.9897	0.0308	0.0126	0.9908	0.0284	0.0117
Logistic	0.9923	0.0258	0.0108	0.9902	0.0316	0.0121	0.9916	0.0282	0.0106
Thompson	0.9872	0.0323	0.0180	0.9818	0.0403	0.0211	0.9892	0.0308	0.0136
Diffusion approach	0.9907	0.0285	0.0129	0.9886	0.0342	0.0139	0.9899	0.0311	0.0128
Modified Henderson and Pabis	0.9914	0.0312	0.0123	0.9897	0.0418	0.0129	0.9906	0.0348	0.0122

[1] M-CD = microwave semi-industrial continuous drying; M-IVD = microwave infrared-vacuum drying; M-IFD = microwave infrared-fluidised bed drying; RMSE = root mean square error.

fluidised bed setups (all with microwave pre-treatment) has the best performance for predicting the drying behaviour of walnut kernel based on selected criteria (Table 2).

Coefficients, drying constants and main indicators of Midilli model for continuous, infrared-vacuum and infrared-fluidised bed arrangements are rendered in Table 3 to 5, respectively. In the following studies, the Midilli model has been suggested as the most appropriate experimental model to predict the drying behaviour in various drying conditions: vacuum drying of shiitake mushroom and chili (Motevali *et al.*, 2012), pineapple, grape and tomato drying under infrared condition (Ponkham *et al.*, 2012), Fluidisation of olive pomace (Ruiz Celma *et al.*, 2009), mushroom slices in hot air-electro-hydrodynamic dryer (Meziane, 2011) and raw olive pomace in convective solar dryer (Taghian Dinani *et al.*, 2014).

Table 3. The statistical comparison, drying constants and coefficients of Midilli model for prediction of drying kinetic of walnut kernel in microwave semi-industrial continuous drying.[1]

Microwave power (W)	Belt speed (mm/s)	Air temperature (°C)	R^2	RMSE	χ^2	a	B	k	n
270	2.5	45	0.9965	0.0171	0.0076	0.9967	-0.031	1.1280	0.9866
		60	0.9982	0.0130	0.0034	0.9904	0.014	1.7550	1.1520
		75	0.9967	0.0180	0.0055	0.9894	-0.025	1.8380	1.0700
	6.5	45	0.9978	0.0135	0.0049	0.9839	-0.092	2.4060	1.1300
		60	0.9976	0.0142	0.0047	0.9935	-0.036	3.2270	1.0310
		75	0.9972	0.0162	0.0050	0.9886	-0.071	3.7730	1.0580
	10.5	45	0.9977	0.0140	0.0053	1.0040	0.021	4.9180	1.1190
		60	0.9983	0.0126	0.0035	0.9960	-4.438	-2.2330	1.3740
		45	0.9979	0.0142	0.0036	0.9782	-0.067	7.4750	1.1880
450	2.5	45	0.9929	0.0260	0.0122	0.9751	0.068	2.5200	1.2040
		60	0.9931	0.0265	0.0099	0.9702	0.041	2.7540	1.1310
		75	0.9918	0.0315	0.0099	0.9700	-2.670	-1.1200	1.2620
	6.5	45	0.9943	0.0212	0.0103	0.9924	0.081	4.0760	0.9538
		60	0.9920	0.0279	0.0117	0.9668	0.108	6.8140	1.1300
		75	0.9914	0.0320	0.0103	0.9696	-0.216	6.6190	1.0870
	10.5	45	0.9959	0.0183	0.0080	0.9827	0.100	6.2480	1.0460
		60	0.9943	0.0232	0.0092	0.9806	0.082	8.7840	1.1360
		45	0.9886	0.0363	0.0145	0.9686	-0.007	14.240	1.2440
630	2.5	45	0.9908	0.0289	0.0133	0.9607	0.006	2.1420	0.9937
		60	0.9884	0.0358	0.0141	0.9454	-2.318	-0.9642	1.2660
		75	0.9824	0.0459	0.0169	0.9547	-0.254	2.0470	0.8842
	6.5	45	0.9894	0.0306	0.0159	0.9749	-0.049	3.9830	0.9894
		60	0.9876	0.0381	0.0160	0.9587	0.059	10.460	1.3420
		75	0.9836	0.0464	0.0151	0.9946	-2.727	0.5004	0.3832
	10.5	45	0.9930	0.0254	0.0103	0.9790	-0.116	6.3140	0.9917
		60	0.9924	0.0279	0.0101	0.9654	0.010	10.530	1.1370
		45	0.9830	0.0483	0.0187	0.9626	-0.143	21.930	1.3440

[1] a, b, c, n are models coefficients and k, g, hare drying constants; RMSE = root mean square error.

Table 4. The statistical comparison, drying constants and coefficients of Midilli model for prediction of drying kinetic of walnut kernel in microwave infrared-vacuum drying.[1]

Microwave power (W)	Absolute pressure (kPa)	Air temperature (°C)	R^2	RMSE	χ^2	a	B	k	n
270	60	45	0.9984	0.0113	0.0038	0.9991	0.042	1.8690	1.0870
		60	0.9961	0.0189	0.0078	1.0020	0.024	2.3240	1.0510
		75	0.9969	0.0188	0.0046	0.9915	0.010	3.6360	1.2580
	40	45	0.9974	0.0157	0.0059	0.9833	0.053	2.4880	1.2790
		60	0.9960	0.0206	0.0072	0.9865	0.062	3.5000	1.3140
		75	0.9931	0.0296	0.0079	0.9828	-0.115	3.9270	1.2510
	20	45	0.9965	0.0190	0.0076	0.9865	0.060	2.8610	1.3720
		60	0.9965	0.0198	0.0055	1.0030	-2.450	-1.0510	1.5480
		45	0.9936	0.0293	0.0069	0.9845	-0.364	3.1510	1.1670
450	60	45	0.9973	0.0152	0.0062	0.9964	0.065	2.4330	1.1560
		60	0.9944	0.0227	0.0093	0.9923	0.032	2.6490	1.0320
		75	0.9897	0.0370	0.0110	0.9864	-2.344	-1.7010	2.7990
	40	45	0.9968	0.0164	0.0062	0.9759	0.062	2.7860	1.0670
		60	0.9927	0.0275	0.0106	0.9776	0.136	5.4280	1.1590
		75	0.9845	0.0495	0.0122	0.9688	-0.278	4.7590	1.1000
	20	45	0.9948	0.0231	0.0085	0.9714	0.099	4.3670	1.2240
		60	0.9914	0.0324	0.0095	0.9720	0.058	5.1290	1.1690
		45	0.9882	0.0452	0.0102	0.9771	-4.045	-2.3300	1.6060
630	60	45	0.9949	0.0197	0.0097	0.9711	-0.019	1.6810	0.9116
		60	0.9905	0.0331	0.0131	0.9675	0.105	5.4570	1.2450
		75	0.9794	0.0609	0.0148	0.9999	-2.711	0.1400	0.1250
	40	45	0.9932	0.0239	0.0126	0.9765	0.051	2.5560	1.0520
		60	0.9885	0.0374	0.0126	0.9679	-0.095	3.8230	1.1370
		75	0.9820	0.0603	0.0145	0.9670	-0.976	4.4580	1.1980
	20	45	0.9913	0.0288	0.0133	0.9733	0.028	2.9820	1.0610
		60	0.9902	0.0347	0.0097	0.9679	-0.492	2.1910	0.9441
		45	0.9752	0.0737	0.0163	0.9991	-2.686	0.3119	0.2814

[1] a, b, c, n are models coefficients and k, g, hare drying constants; RMSE = root mean square error.

Shrinkage

Figure 4 demonstrates the effects of drying conditions on shrinkage coefficient in M-CD, M-IVD, and M-IFD domains, respectively. Values of shrinkage (S_b) in different drying conditions were calculated using Equation 5. In all experimental arrangements, maximum values of shrinkage were observed at the highest drying temperature and microwave power. In walnut kernel drying, as drying temperature and microwave power increased, the moisture diffusion increased leading to the shrinkage increment. In the other words, during all drying processes due to the water loss of foodstuff and increased moisture diffusion in any biological material, the food is out of balance and a pressure differential is generated between the inside and outside of the material. The pressure imbalance makes deformation and cracking then reducing the volume of the product (Alaei and Chayjan, 2015).

Based on key results, minimum shrinkage in M-CD (6.53%) was related to the microwave power of 270 W, air temperature of 45 °C and belt linear speed of 10.5 mm/s (in belt higher speeds, sample exposure time to the hot air diminished causing the least shrinkage). Maximum shrinkage (11.55%) belonged to the microwave power of 630 W, air temperature of 75 °C, and belt linear speed of 2.5 mm/s.

In M-IVD domain, the maximum shrinkage (14.65%) was achieved at the microwave power of 630 W, drying

Table 5. The statistical comparison, drying constants and coefficients of Midilli model for prediction of drying kinetic of walnut kernel in microwave infrared-fluidised bed drying.[1]

Microwave power (W)	Infrared radiation (W)	Air temperature (°C)	R^2	RMSE	χ^2	a	B	k	n
270	500	45	0.9982	0.0118	0.0033	0.9852	-0.009	1.7430	0.9241
		60	0.9972	0.0157	0.0047	0.9747	0.041	2.7790	1.0440
		75	0.9913	0.0288	0.0125	0.9365	-2.518	-1.0990	1.2770
	1000	45	0.9932	0.0251	0.0119	0.9776	-2.151	-0.8579	1.2590
		60	0.9945	0.0237	0.0084	0.9725	-2.421	-0.9922	1.2770
		75	0.9955	0.0230	0.0053	0.9845	-0.348	2.1340	0.9652
	1,500	45	0.9966	0.0178	0.0051	0.9884	-0.143	1.7710	0.9704
		60	0.9928	0.0297	0.0088	0.9792	0.002	4.4440	1.2120
		45	0.9938	0.0289	0.0067	0.9827	-0.232	3.6140	1.0780
450	500	45	0.9963	0.0181	0.0072	0.9641	0.051	2.6040	1.1930
		60	0.9951	0.0211	0.0080	0.9767	0.011	2.6390	1.0160
		75	0.9952	0.0216	0.0070	0.9731	0.016	3.1030	0.9897
	1000	45	0.9951	0.0211	0.0076	0.9704	0.026	2.8590	1.0230
		60	0.9920	0.0293	0.0103	0.9749	-0.018	3.3530	1.0020
		75	0.9898	0.0357	0.0115	0.9745	0.066	5.2350	1.0790
	1,500	45	0.9899	0.0333	0.0133	0.9620	0.052	4.3230	1.2040
		60	0.9910	0.0331	0.0099	0.9696	0.080	5.2030	1.0930
		45	0.9888	0.0402	0.0113	0.9624	0.182	9.0120	1.2330
630	500	45	0.9930	0.0249	0.0130	0.9671	0.039	2.5830	1.1050
		60	0.9926	0.0263	0.0110	0.9645	0.021	2.9170	1.0640
		75	0.9926	0.0275	0.0098	0.9652	0.055	3.8240	1.0920
	1000	45	0.9902	0.0314	0.0148	0.9717	0.082	3.9390	1.1590
		60	0.9906	0.0332	0.0122	0.9661	0.060	4.9760	1.1940
		75	0.9835	0.0474	0.0157	0.9706	-0.069	4.6560	1.0680
	1,500	45	0.9893	0.0345	0.0143	0.9717	-0.002	3.7210	1.1170
		60	0.9812	0.0493	0.0194	0.9700	-0.047	4.3810	1.0140
		45	0.9772	0.0590	0.0209	0.9591	-0.060	5.8760	1.0930

[1] a, b, c, n are models coefficients and k, g, hare drying constants; RMSE = root mean square error.

temperature of 75 °C, and absolute pressure of 60 kPa; however, the minimum value (8.26%) was obtained in the condition of 630 W, 75 °C and 20 kPa. In lower absolute pressures, the associated saturated temperature of the water inside the material reduced, as well. This phenomenon terminated to the rapid water evaporation, increase in the drying rate, and reduction in the drying time, which eventually caused lower shrinkage. In M-IFD, microwave power of 270 W, air temperature of 45 °C and infrared radiation of 500 W yielded the minimum shrinkage (6.72%) and the microwave power of 630 W, temperature of 75 °C and radiant power of 1,500 W resulted in the maximum shrinkage coefficient (13.50%). By increasing the radiant power from 500 up to 1,500 W the sample absorbs more infrared radiation, the intracellular water is heated and evaporation increases causing more shrinkage.

According to Figure 4, in all experimental domains the effect of air temperature on shrinkage was more pronounced compared to other conditions. Equations 17 to 19 presented the quadratic mathematical models followed by their coefficient of determination (R^2) proposed for walnut kernel shrinkage in M-CD, M-IVD, and M-IFD domains, respectively. These equations explain the relation between S_b and other independent variables (air temperature, microwave power, etc.) as follows:

$$S_b = 3.21 + 0.043T + 2.49\times10^{-3}P_{MW} - 0.068u_b - 5.91\times10^{-6}TP_{MW} + 7.65\times 10^{-5}Tu_b + 2.90\times10^{-5}P_{MW}u_b + 7.75\times10^{-4}T^2 - 1.14\times10^{-6}P_{MW}^2 - 4.34\times10^{-4}u_b^2 \quad , \quad R^2=0.9978 \quad (17)$$

$$S_b = -1.55 + 0.22\,T + 1.66\times10^{-3}P_{MW} - 1.47\times10^{-3}P_V + 5.66\times10^{-6}TP_{MW} - 4.34\times 10^{-5}TP_V + 5.60\times10^{-6}P_{MW}P_V - 3.15\times10^{-4}T^2 - 1.79\times10^{-7}P_{MW}^2 + 9.46\times10^{-5}P_v^2 \quad , \quad R^2=0.9995 \quad (18)$$

$$S_b = -9.09 + 0.48T - 4.47\times10^{-3}P_{MW} - 4.46\times10^{-4}P_{IR} + 8.23\times10^{-5}TP_{MW} + 1.04\times 10^{-5}TP_{IR} + 3.45\times10^{-7}P_{MW}P_{IR} - 2.83\times10^{-3}T^2 + 1.64\times10^{-6}P_{MW}^2 - 1.36\times10^{-8}P_{IR}^2 \quad , \quad R^2=0.9996 \quad (19)$$

Where T is the inlet air temperature (°C), P_{MW} is the microwave power (W), u_b is the belt linear speed (mm/s), P_V is the absolute pressures (kPa) and P_{IR} is the infrared power (W).

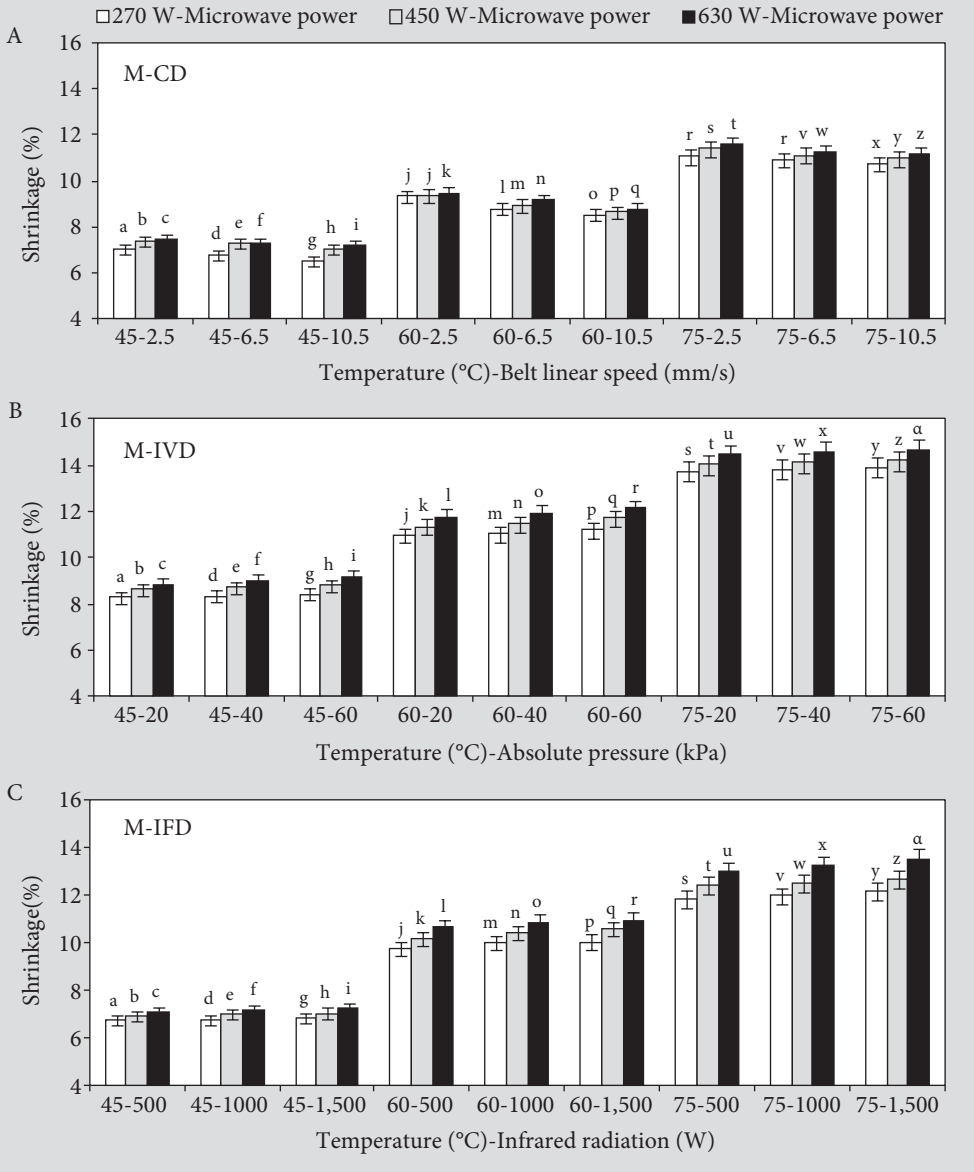

Figure 4. Shrinkage values of walnut kernel at different drying temperatures in: microwave semi-industrial continuous drying (M-CD) (A), microwave infrared-vacuum drying (M-IVD) (B) and microwave infrared-fluidised bed drying (M-IFD) (C).

Colour

Calculations of the specific colour values (L^*, a^*, and b^*) were conducted by the Equations 6 to 8 and total colour change (ΔE) of the walnut kernel was then determined using the Equation 9 after drying. Figures 5 shows the values of ΔE for all experiments conducted in all dryers, comparatively. As can be seen from the figures, the highest total colour change was obtained at the microwave power of 630 W and air temperature of 75 °C; however, the lowest value of ΔE belonged to the microwave power of 270 W and air temperature of 45 °C. Augmentation in drying air temperature and microwave power generated browning reactions, which resulted in an increment in the surface and superficial burns of walnut kernel.

In M-CD of the walnut kernel, maximum (18.28%) and minimum (8.27%) values of ΔE were achieved at belt linear speeds of 10.5 and 2.5 mm/s, respectively. In M-IVD, the minimum (5.54%) and maximum (13.90%) values of ΔE were related to the absolute pressures of 20 and 60 kPa, respectively. Under equal conditions, in lower values of absolute pressure, drying time was reduced and samples received less heat, resulting in less total colour changes. Under M-IFD, the maximum (16.73%) and minimum (6.10%) values of ΔE belonged to the radiant powers of 1,500 and 500 W, respectively. In higher infrared radiations, the

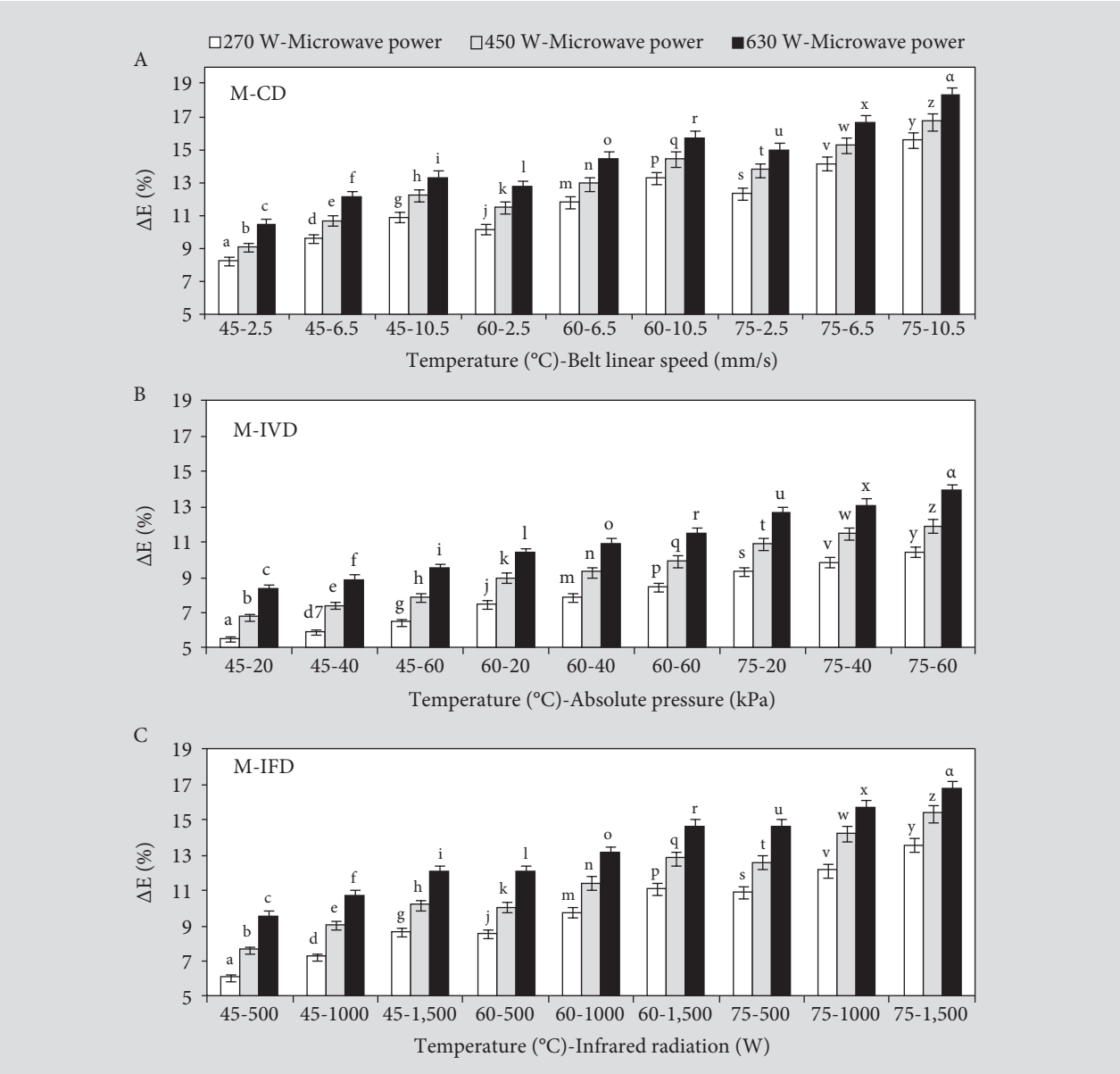

Figure 5. Total colour difference (Δ*E*) of walnut kernel at different drying conditions in: microwave semi-industrial continuous drying (M-CD) (A), microwave infrared-vacuum drying (M-IVD) (B) and microwave infrared-fluidised bed drying (M-IFD) (C).

walnut samples absorbed more infrared radiation causing the superficial burns and colour changes in walnut kernel. Similar results were reported in other studies such as: sorbus fruits drying in convective-microwave arrangement in which by increase in drying air temperature, total colour change increased, as well (Lüle and Koyuncu, 2015), grape (Mohebbi *et al.*, 2009) and red ginseng drying in infrared dryer (Behroozi-Khazaei *et al.*, 2013). By the combination of infrared and microwave powers in green pepper drying, total colour change reduced (Ning *et al.*, 2015). The total colour change in the kiwifruit decreased in a vacuum dryer in comparison with hot air drying (Lechtanska *et al.*, 2015). ΔE of jujube fruit subjected to the hot air drying was reported more than the ΔE value obtained from infrared drying under the fixed drying air temperature (Orikasa *et al.*, 2014). By increasing the mushroom exposure time to the infrared radiation, ΔE value increased (Chen *et al.*, 2015).

Equations 20 to 22 presented the mathematical models and related R^2 suggested for calculating of walnut kernel total colour change (ΔE) in M-CD, M-IVD, and M-IFD, respectively as follows:

$$\Delta E = 0.24 + 0.14T + 1.54\times10^{-3}P_{MW} + 0.26u_b + 3.32\times10^{-5}TP_{MW} + 2.11\times10^{-3}Tu_b + 5.40\times10^{-5}P_{MW}u_b - 1.47\times10^{-4}T^2 + 3.48\times10^{-6}P_{MW}^2 - 3.15\times10^{-3}u_b^2,\ R^2 = 0.9959 \quad (20)$$

$$\Delta E = -0.61 + 0.076T + 4.88\times10^{-3}P_{MW} - 5.25\times10^{-4}P_V + 3.97\times10^{-5}TP_{MW} + 1.40\times10^{-4}TP_V + 1.01\times10^{-5}P_{MW}P_V + 3.08\times10^{-4}T^2 + 1.15\times10^{-6}P_{MW}^2 + 1.78\times10^{-4}P_V^2,\ R^2 = 0.9991 \quad (21)$$

$$\Delta E = -3.89 + 0.089T + 0.012P_{MW} + 3.42\times10^{-3}P_{IR} - 3.05\times10^{-6}TP_{MW} - 4.01\times10^{-6}TP_{IR} - 9.08\times10^{-7}P_{MW}P_{IR} + 6.75\times10^{-4}T^2 - 1.37\times10^{-6}P_{MW}^2 - 1.22\times10^{-7}P_{IR}^2,\ R^2 = 0.9950 \quad (22)$$

Effective moisture diffusivity

The plot of effective moisture diffusivity (D_{eff}) versus different drying conditions in all experimental domains are presented in Figure 6. Values of the walnut effective moisture diffusivity were calculated using Equation 12 at different drying conditions. During the drying process, existing of capillary tubes, pores, and air-filled holes in food materials causes movement of water vapour and moisture from inside to the outside surfaces of the material. By increasing the air temperature and microwave power, heating energy increased causing an increment in the activity of water molecules, therefore, the volume of water vapour transmission increased, resulting in increased diffusivity. So that in all arrangements, the maximum values of effective moisture diffusivity was related to the microwave power of 630 W and drying temperature of 75 °C, and the minimum value belonged to the 270 W and 45 °C. Diffusivity values of the walnut samples varied within the range of 1.04×10^{-8} to 6.01×10^{-8} m^2/s, which was consistent with the effective moisture diffusivity of bio-products (often in the order of 10^{-8} to 10^{-12} m^2/s) (Alaei and Chayjan, 2015). In M-CD, the minimum moisture diffusivity (1.04×10^{-8} m^2/s) was obtained at the belt linear speed of 2.5 mm/s and the maximum value (9.74×10^{-8} m^2/s) was achieved at the belt linear speed of 10.5 mm/s. In higher belt linear speeds due to the long exposing time of samples to the microwave radiation, the effective moisture diffusivity increased, as well. In M-IVD, the minimum value of diffusivity (1.18×10^{-8} m^2/s) was achieved in the absolute pressure of 60 kPa; however, the maximum value (6.01×10^{-8} m^2/s) was obtained at 20 kPa. In lower absolute pressures, increased suction pressure in drying chamber would help to rapid movement of internal water of walnut kernel toward the surface through the pores. In M-IFD domain, the minimum diffusivity (1.37×10^{-8} m^2/s) belonged to the radiant power of 500 W. The maximum value (4.46×10^{-8} m^2/s) was related to the 1,500 W. As radiant power increased, the heating energy increased as well, it caused temperature gradient between inside and outside of the material, leading to the augmentation in moisture diffusivity.

The mathematical models proposed for effective moisture diffusivity (D_{eff}) of walnut kernel in M-CD, M-IVD and M-IFD, respectively as follows:

$$D_{eff} = 6.86\times10^{-8} - 1.93\times10^{-9}T - 8.15\times10^{-11}P_{MW} - 1.57\times10^{-9}u_b + 1.28\times10^{-12}TP_{MW} + 8.67\times10^{-11}Tu_b + 9.18\times10^{-12}P_{MW}u_b + 1.24\times10^{-11}T^2 + 7.50\times10^{-15}P_{MW}^2 - 2.02\times10^{-10}u_b^2,\ R^2 = 0.9793 \quad (23)$$

$$D_{eff} = 9.72\times10^{-8} - 2.63\times10^{-9}T - 1.03\times10^{-10}P_{MW} - 4.56\times10^{-11}P_V + 2.01\times10^{-12}TP_{MW} - 1.17\times10^{-12}TP_V - 4.71\times10^{-14}P_{MW}P_V + 2.21\times10^{-11}T^2 + 2.62\times10^{-14}P_{MW}^2 - 1.20\times10^{-12}P_V^2,\ R^2 = 0.9895 \quad (24)$$

$$D_{eff} = 3.85\times10^{-9} - 1.73\times10^{-10}T + 3.91\times10^{-11}P_{MW} - 6.15\times10^{-12}P_{IR} - 2.40\times10^{-15}TP_{MW} + 2.89\times10^{-13}TP_{IR} + 1.51\times10^{-14}P_{MW}P_{IR} + 2.51\times10^{-12}T^2 - 4.16\times10^{-14}P_{MW}^2 - 2.63\times10^{-15}P_{IR}^2,\ R^2 = 0.9954 \quad (25)$$

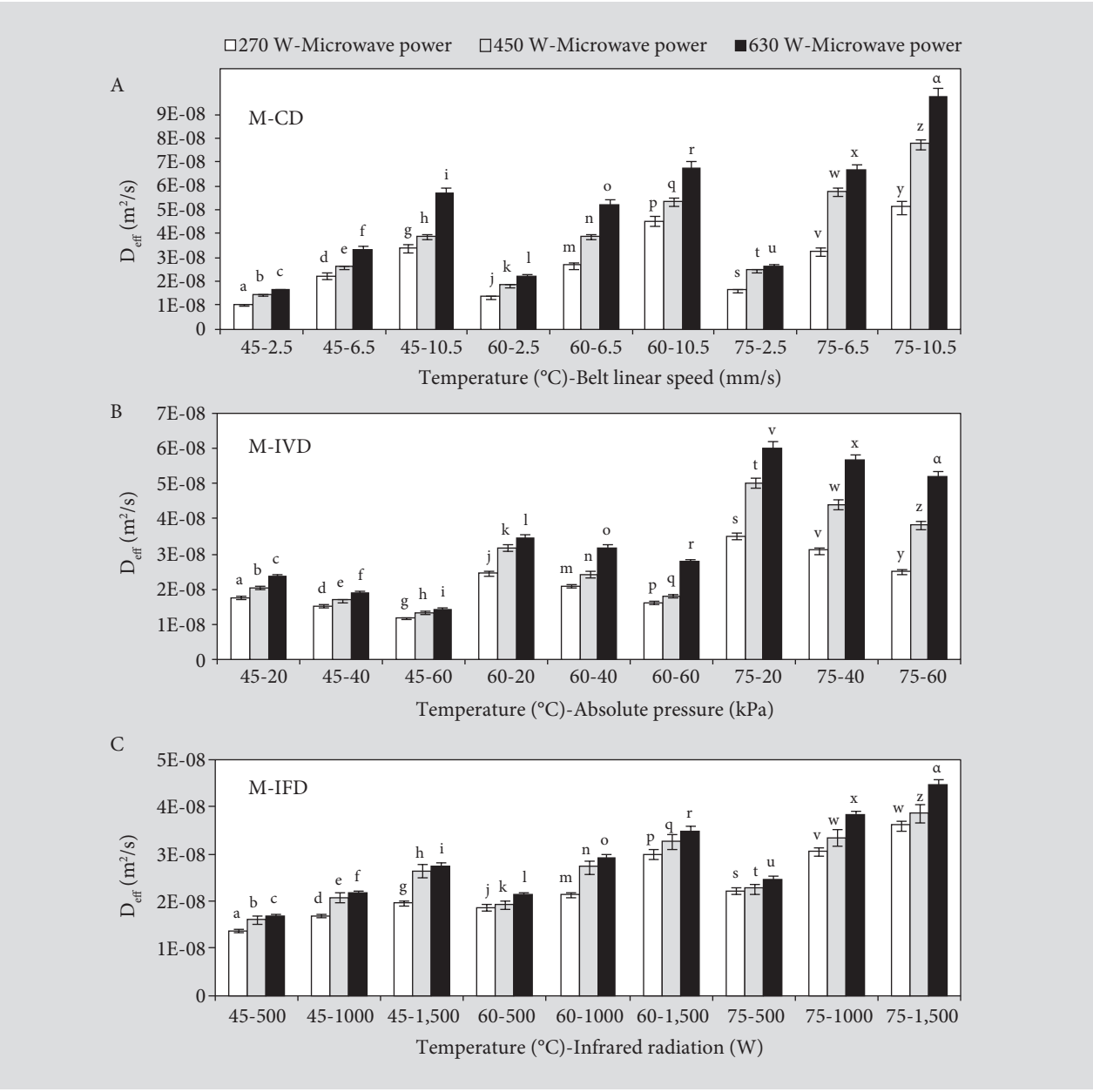

Figure 6. Effective moisture diffusivity (D_{eff}) of walnut kernel in microwave semi-industrial continuous drying (M-CD) (A), microwave infrared-vacuum drying (M-IVD) (B) and microwave infrared-fluidised bed drying (M-IFD) (C).

Activation energy

Different values of activation energy (E_a) and correlation coefficients (R^2) of the walnut kernel at different drying conditions associated to all arrangements are rendered in Table 6. To calculate the activation energy from the slope of the Arrhenius equation (Equations. 15 and 16), the simple plots of ln (D_{eff}) against the inverse of absolute air temperatures ($1/T_a$) are shown in Supplementary Figure S4 for various experimental domains.

According to Table 6, the E_a values of the walnut kernel in M-CD, M-IVD, and M-IFD were achieved between 11.58 to 24.52 kJ/mol, 20.99 to 39.55 kJ/mol and 10.52 to 20.65 kJ/mol, respectively. E_a values of different agricultural products were within the range of 12 to 110 kJ/mol (Alaei and Chayjan, 2015). Based on results, in M-CD arrangement, at fixed belt linear speed (within the study range) the activation energy of walnut kernel in the microwave power of 450 W was more than values in the powers of 270 and 630 W. In the M-IVD domain, at the same absolute pressures with an increase in the microwave power from 270 to 630 W, values of activation energy increased, as well. In M-IFD, at a constant radiant power the values of E_a in microwave power of 450 W was found to be less than the values in the microwave powers of 270 and 630

Table 6. Activation energy values (E_a) and related correlation coefficients (R^2) of walnut kernel.

Dryer type	Microwave power (W)								
	270			450			630		
Semi-industrial continuous									
Belt speed (mm/s)	2.5	6.5	10.5	2.5	6.5	10.5	2.5	6.5	10.5
E_a (kJ/mol)	13.692	11.584	12.387	16.449	24.524	21.231	14.482	21.148	16.360
R^2	0.9931	0.9957	0.9575	0.9958	0.9990	0.9953	0.9849	0.9794	0.9460
Vacuum									
Absolute pressure (kPa)	60	40	20	60	40	20	60	40	20
E_a (kJ/mol)	23.066	21.625	20.991	31.845	29.229	27.344	39.551	33.404	28.598
R^2	0.9861	0.9918	0.9967	0.9300	0.9737	0.9986	1.0000	0.9964	0.9820
Infrared									
Infrared radiation (W)	500	1000	1,500	500	1000	1,500	500	1000	1,500
E_a (kJ/mol)	14.807	20.648	18.839	10.518	14.632	11.534	11.689	17.514	14.849
R^2	0.9808	0.9964	0.9610	0.9998	0.9973	0.9986	0.9894	0.9999	0.9990

W. Considering identical cultivar, species, initial moisture content, and storage condition for all walnut samples, the differences in the activation energy values is not only due to the difference between various drying conditions but also to the individual performance of each experimental set up. The value of activation energy depends strongly on the chemical structure and moisture content of food product (Wang *et al.*, 2015). According to the results and due to the high volume of the moisture content of walnut kernel, the E_a values obtained are less than a lot of food materials.

4. Conclusions

This study was performed to evaluate and modelling of some physical and thermal properties of walnut kernel under different drying conditions. Maximum and minimum drying time (about 100 and 11 min) were related to the M-CD domain achieving at the air temperatures of 45 and 75 °C, microwave powers of 270 and 630 W and belt linear speeds of 2.5 and 10.5 mm/s, respectively. Midilli model was the best describing drying behaviour with R^2=0.9927 for continuous, R^2=0.9918 for M-IVD, and R^2=0.9917 for M-IFD. Minimum values of shrinkage (6.53%) and ΔE (5.54%) were related to the microwave power of 270 W, drying temperature of 45°C, and belt linear speed of 10.5 mm/s in M-CD, however maximum values of shrinkage (14.65%) and ΔE (18.28%) were obtained at microwave power of 630 W, air temperature of 75 °C, and absolute pressure of 60 kPa in M-IVD domain. The minimum and maximum values of effective moisture diffusivity (1.04×10^{-8} and 9.74×10^{-8} m^2/s) were obtained in M-CD arrangement. The maximum value of activation energy (39.55 kJ/mol) was achieved in M-IVD however, the minimum activation energy (10.52 kJ/mol) was related to the M-IFD and M-CD set of connections, respectively. In the viewpoints of research dependents including drying kinetics and quality indices (shrinkage and colour) the M-CD domain was recommended as the most appropriate technique amongst applied arrangements in walnut kernel drying. Under specific drying conditions, the very short time of drying process can be an economic factor and incentive for the application of M-CD heat processing method on an industrial scale for other nuts, fruits, and vegetables.

Supplementary material

Supplementary material can be found online at https://doi.org/10.3920/QAS2017.1071.

Figure S1. Moisture ratio of walnut kernel versus time at three drying in microwave semi-industrial continuous drying.

Figure S2. Moisture ratio of walnut kernel versus time at three drying in microwave infrared-vacuum drying.

Figure S3. Moisture ratio of walnut kernel versus time at three drying temperatures in microwave infrared-fluidised bed drying.

Figure S4. Ln effective moisture diffusity (D_{eff}) against $1/t_a$ at different conditions for drying of walnut kernel in microwave semi-industrial continuous drying, microwave infrared-vacuum drying and microwave infrared-fluidised bed drying.

References

Aghbashlo, M., Kianmehr, M.H., Arabhosseini, A. and Nazghelichi, T., 2011. Modelling the carrot thin-layer drying in a semi-industrial continuous band dryer. Czech Journal of Food Science 29(5): 528-538.

Ahrne, L., Prothon, F. and Funebo, T., 2003. Comparison of drying kinetics and texture effects of two calcium pretreatments before microwave-assisted dehydration of apple and potato. International Journal of Food Science and Technology 38: 411-420.

Aidani, E., Hadadkhodaparast, M. and Kashaninejad, M., 2016. Experimental and modeling investigation of mass transfer during combined infrared-vacuum drying of Hayward kiwifruits. Food Science and Nutrition 5(3): 596-601.

Alaei, B. and Chayjan, R.A., 2015. Drying characteristics of pomegranate arils under near infrared-vacuum conditions. Journal of Food Processing Preservation 39(5): 469-479.

Aregbesola, O.A., Ogunsina, B.S., Sofolahan, A.E. and Chime, N.N., 2015. Mathematical modeling of thin layer drying characteristics of dika (*Irvingia gabonensis*) nuts and kernels. Nigerian Food Journal 33(1): 83-89.

Behroozi-Khazaei, N., Tavakoli Hashjin, T., Ghassemian, H., Khoshtaghaza, M. and Banakar, A., 2013. Application of machine vision in modeling of grape drying process. Journal of Agricultural Science Technology 15: 1095-1106.

Chen, Q., Bi, J., Wu, X., Yi, J., Zhou, L. and Zhou, Y., 2015. Drying kinetics and quality attributes of jujube (Zizyphus jujuba Miller) slices dried by hot-air and short- and medium-wave infrared radiation. LWT-International Journal of Food Science Technology 64(2): 759-766.

Clary, C.D., Wang, S.J. and Petrucci, V.E., 2005. Fixed and incremental levels of microwave power application on drying grapes under vacuum. Journal of Food Science 70(5): 344-349.

Crank, J., 1997. The mathematics of diffusion, 2nd edition. Clarendon Press, Oxford, UK.

Cui, Z.W., Xu, S.Y. and Sun, D.W., 2005. Temperature changes during microwave-vacuum drying of sliced carrots. Drying Technology 23: 1057-1074.

Darrigues, A., Hall, J., Van Der Knaap, E., Francis, D.M., Dujmovic, N. and Gray, S., 2008. Tomato analyzer-color test: a new tool for efficient digital phenotyping. Journal of the American Society for Horticultural Science 133(4): 579-586.

Dash, K.K., Gope, S., Sethi, A. and Doloi, M., 2013. Study on thin layer drying characteristics star fruit slices. International Journal Agriculture and Food Science Technology 4(7): 679-686.

Durance, T.D. and Wang, J.H., 2002. Energy consumption, density and rehydration rate of vacuum microwave- and hot-air convection-dehydrated tomatoes. Journal of Food Science 67: 2212-2216.

Faal, S., Tavakoli, T. and Ghobadian, B., 2015. Mathematical modelling of thin layer hot air drying of apricot with combined heat and power dryer. Journal of Food Science and Technology 52(5): 2950-2957.

Food and Agriculture Organisation (FAO), 2012. Corporate document repository. Available at: http://faostat.fao.org.

Ghatrehsamani, S.H. and Zomorodian, A., 2012. Impacts of drying air temperature, bed depth and air flow rate on walnut drying rate in an indirect solar dryer. International Journal of Agriculture Sciences 4(6): 253.

Gogus, F. and Maskan, M., 2001. Drying of olive pomace by a combined microwave-fan assisted convection oven. Nahrung 45(2): 129-132.

Gonçalves, L.T., Pereira, N.R., Almeida, S.B., Freitas, S.D.J. and Waldman, W.R., 2016. Microwave-hot air drying applied to selected cassava cultivars: drying kinetics and sensory acceptance. International Journal of Food Science and Technology 52(2): 389-397.

Janjai, S., Mahayothee, B., Lamlert, N., Bala, B.K., Precoppe, M., Nagle, M. and Müller, J., 2010. Diffusivity, shrinkage and simulated drying of litchi fruit (*Litchi Chinensis Sonn.*). International Journal of Food Engineering 96(2): 214-221.

Kashaninejad, M., Mortazavi, A., Safekordi, A. and Tabil, L.G., 2007. Thin-layer drying characteristics and modeling of pistachio nuts. International Journal of Food Engineering 78(1): 98-108.

Khadivi-Khub, A., Ebrahimi, A., Sheibani, F. and Esmaeili, A., 2015. Phenological and pomological characterization of Persian walnut to select promising trees. Euphytica 205(2): 557-567.

Kouchakzadeh, A., 2013. The effect of acoustic and solar energy on drying process of pistachios. Energy Conversion and Management 67: 351-356.

Koukouch, A,. Idlimam, A., Asbik, M., Sarh, B., Izrar, B., Bah, A. and Ansari, O., 2015. Thermo physical characterization and mathematical modeling of convective solar drying of raw olive pomace. Energy Conversions and Management 99: 221-230.

Lechtanska, J.M., Szadzińska, J. and Kowalski, S.J., 2015. Microwave-infrared-assisted convective drying of green pepper: quality and energy considerations. Chemical Engineering Process: Process Intensification 98: 155-164.

Lüle, F. and Koyuncu, T., 2015. Convective and microwave drying characteristics of sorbus fruits *(Sorbus domestica* L.). Procedia – Social and Behavioral Sciences 195(3): 2634-2643.

Maskan, M., 2001. Kinetics of colour change of kiwifruits during hot air and microwave drying. Journal of Food Engineering 48: 169-175.

Meziane, S., 2011. Drying kinetics of olive pomace in a fluidized bed dryer. Energy Conversion and Management 52(3): 1644-1649.

Mohebbi, M., Akbarzadeh, M.R.T., Shahidi, F., Moussavi, M. and Ghoddusi, H.B., 2009. Computer vision systems (CVS) for moisture content estimation in dehydrated shrimp. Computers and Electronics in Agriculture 69(2): 128-134.

Monteiro, R.L., Carciofi, B.A.M., Marsaioli, A. and Laurindo, J.B., 2015. How to make a microwave vacuum dryer with turntable. International Journal of Food Engineering 166: 276-284.

Motevali, A., Abbaszadeh, A., Minaei, S., Khoshtaghaza, M.H. and Ghobadian, B., 2012. Effective moisture diffusivity, activation energy and energy consumption in thin-layer drying of Jujube in thin-layer drying of Jujube (*Zizyphus jujube Mill*). Journal of Agricultural Science and Technology 14(3): 523-532.

Ning, X., Lee, J. and Han, C., 2015. Drying characteristics and quality of red ginseng using far-infrared rays. Journal of Ginseng Research 39(4): 371-375.

Nowacka, M., Wiktor, A., Śledź, M., Jurek, N. and Witrowa-Rajchert, D., 2012. Drying of ultrasound pretreated apple and its selected physical properties. International Journal of Food Engineering 113(3): 427-433.

Orikasa, T., Koide, S., Okamoto, S., Imaizumi, T., Muramatsu, Y., Takeda, J.I., Shiina, T. and Tagawa, A., 2014. Impacts of hot air and vacuum drying on the quality attributes of kiwifruit slices. International Journal of Food Engineering 125: 51-58.

Pollegioni, P., Woeste, K.E., Chiocchini, F., Olimpieri, I., Tortolano, V., Clark, J., Hemery, G.E., Mapelli, S. and Malvolti, M.E., 2014. Landscape genetics of Persian walnut (*Juglans regia L.*) across its Asian range. Tree Genetics and Genomes 10(4): 1027-1043.

Ponkham, K., Meeso, N., Soponronnarit, S. and Siriamornpun, S., 2012. Modeling of combined far-infrared radiation and air drying of a ring shaped-pineapple with/without shrinkage. Food and Bioproducts Processing 90(2): 155-164.

Rodriguez, R. and Lombranna, J.I., 2007. Moisture diffusivity analysis in a microwave drying process under different operating conditions. Drying Technology 25(11): 1875-1883.

Rodriguez, R., Lombrana, J.I., Kamel, M. and De Elvira, C., 2005. Kinetic and quality study of mushroom drying under microwave and vacuum. International Journal of Drying Technology 23(9-11): 2197-2213.

Rudy, S., Dziki, D., Krzykowski, A., Gawlik-Dziki, U., Polak, R., Różyło, R. and Kulig, R., 2015. Influence of pre-treatments and freeze-drying temperature on the process kinetics and selected physico-chemical properties of cranberries (*Vaccinium macrocarpon* Ait.). LWT – International Journal of Food Science and Technology 63(1): 497-503.

Ruiz Celma, A., Cuadros, F. and López-Rodríguez, F., 2009. Characterisation of industrial tomato by-products from infrared drying process. Food and Bioproducts Processing 87(4): 282-291.

Siqueira, V.C., Resende, O. and Chaves, T.H., 2012. Drying kinetics of Jatropha seeds. Revista Ceres 59(2): 171-177.

Taghian Dinani, S., Hamdami, N., Shahedi, M. and Havet, M., 2014. Mathematical modeling of hot air/electrohydrodynamic (EHD) drying kinetics of mushroom slices. Energy Conversation and Management 86: 70-80.

Togrul, H. and Arslan, N., 2007. Moisture sorption isotherms and thermodynamic properties of walnut kernels. Journal of Stored Products Research 43(3): 252-264.

United States Department of Agriculture (USDA), 2015. National nutrient database for standard reference release 28. Available at: http://ndb.nal.usda.gov/ndb/foods/show/3720.

Wang, H.C., Zhang, M. and Adhikari, B., 2015. Drying of shiitake mushroom by combining freeze-drying and mid-infrared radiation. Food Bioproduct Process 94: 507-517.

Wang, J. and Sheng, K., 2006. Far infrared and microwave drying of peach. LWT-International Journal of Food Science and Technology 39(3): 247-255.

Zhang, M., Tang, J., Mujumdar, A.S. and Wang, S., 2006. Trends in microwave-related drying of fruits and vegetables. International Journal of Food Science and Technology 17(10): 524-534.